

Electronic Supplementary Information

Simultaneous pre-intercalation of caesium and sodium ions into vanadium oxide bronze nanowires for high-performance aqueous zinc-ion batteries

Hua Tian, Yunyi He, Lin Wang,* Yuannan Lai, Jianwei Wang, Hanqing Xiang, Wenjun Zhao and Lin Zhang*

Hebei Key Laboratory of Applied Chemistry, Hebei Key Laboratory of Heavy Metal Deep-Remediation in Water and Resource Reuse, College of Environmental and Chemical Engineering, Yanshan University, Qinhuangdao, 066004, China

Corresponding authors. E-mail: chinalinkwang@126.com (L. Wang); zhangl2013@ysu.edu.cn (L. Zhang).

Calculation of the solid diffusion coefficient:

The solid diffusion coefficient was calculated using the equation as follows:¹

$$D = \frac{4L^2}{\pi\tau} \left\{ \frac{\Delta E_s}{\Delta E_t} \right\}^2$$

where t represents the duration of the current pulse (s), τ is the relaxation time (s), and ΔE_s means the steady-state potential change (V) by the current pulse. ΔE_t is the potential change (V) during the constant current pulse after eliminating the iR drop. L is the ion diffusion distance (cm), and the electrode thickness is often used to express its value.

Table S1 The interplanar spacing of vanadium oxide bronzes from XRD patterns

Sample	<i>d</i> -spacing (Å)								
	<i>d</i> ₀₀₁	<i>d</i> ₁₀₀	<i>d</i> ₀₀₂	<i>d</i> ₂₀₀	<i>d</i> ₀₀₄	<i>d</i> ₁₁₋₁	<i>d</i> ₁₀₄	<i>d</i> ₀₁₃	<i>d</i> ₁₀₆
NVO	/	9.342	7.178	4.702	3.598	3.354	3.050	2.902	2.170
NCVO	14.482	9.481	7.241	4.741	3.621	3.370	3.063	2.912	2.175

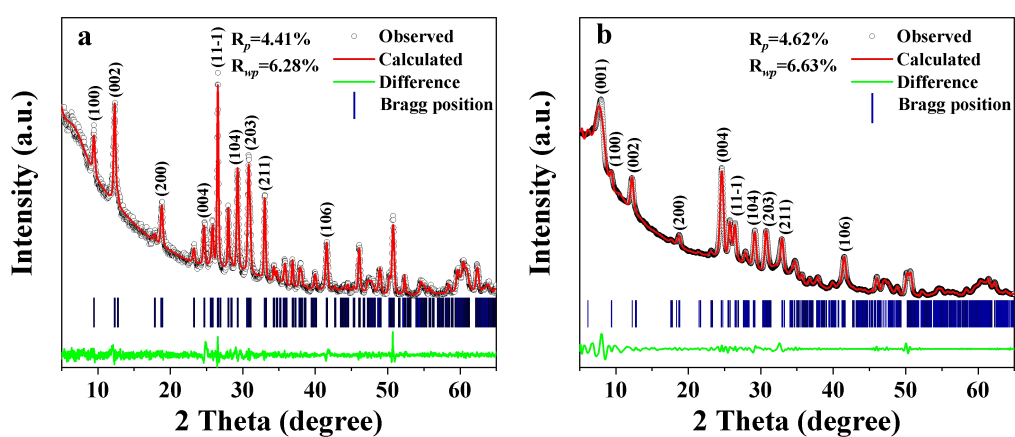


Fig. S1 The Rietveld refinements of vanadium oxide bronzes: (a) NVO. (b) NCVO.

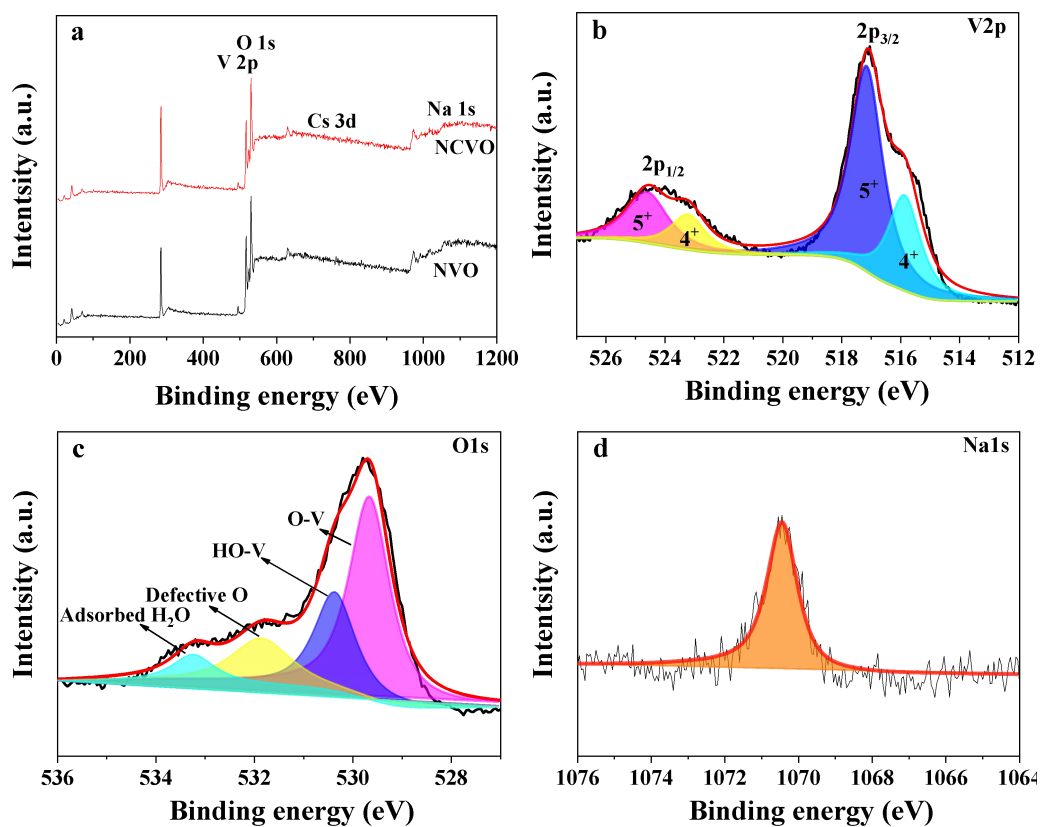


Fig. S2 XPS spectra of NVO: (a) XPS survey spectra of NVO and NCVO. (b) High-resolution V 2p XPS spectrum. (c) High-resolution O 1s XPS spectrum. (d) High-resolution Na 1s XPS spectrum.

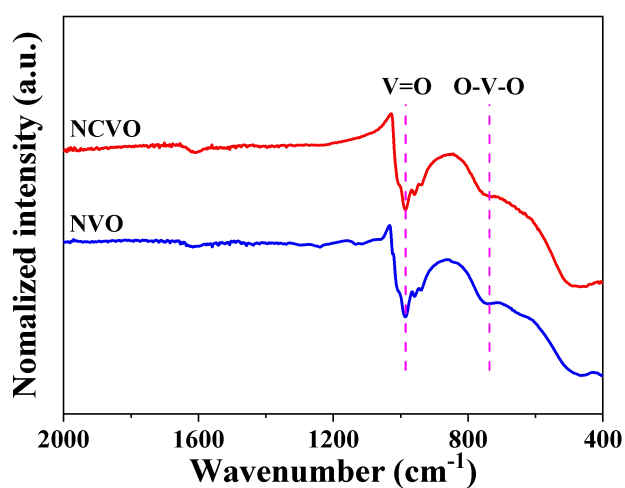


Fig. S3 FT-IR spectra of vanadium oxide bronzes

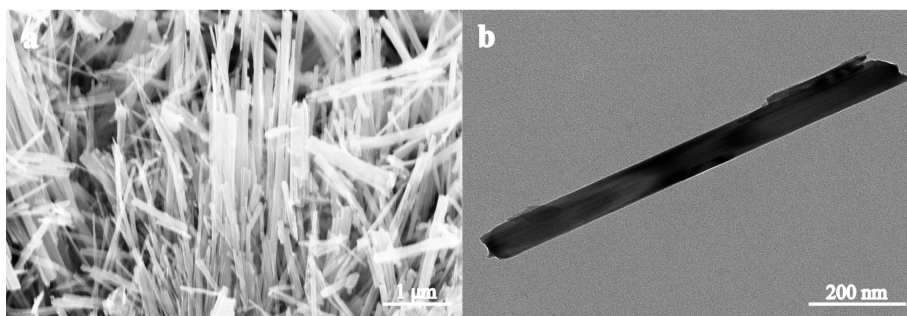


Fig. S4 Morphological characterizations of NVO: (a) SEM image. (b) TEM image.

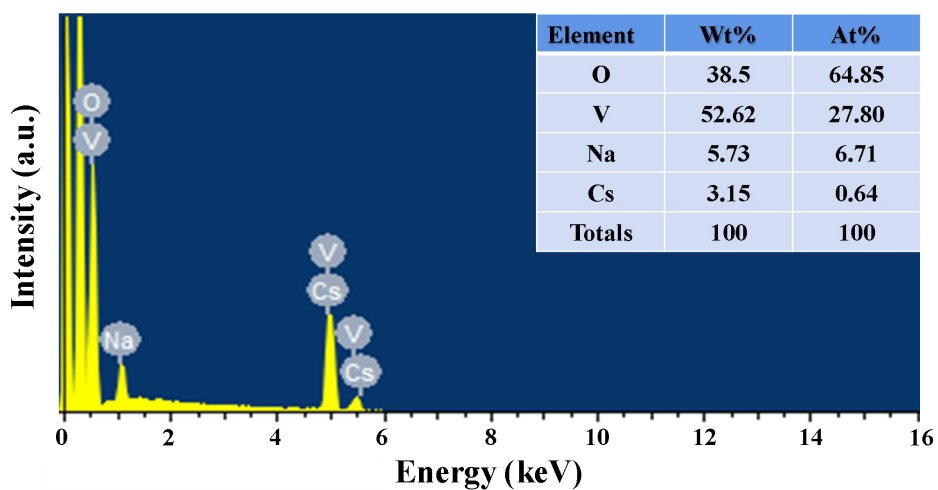


Fig. S5 Corresponding EDS spectrum of NCVO from the element mapping distribution.

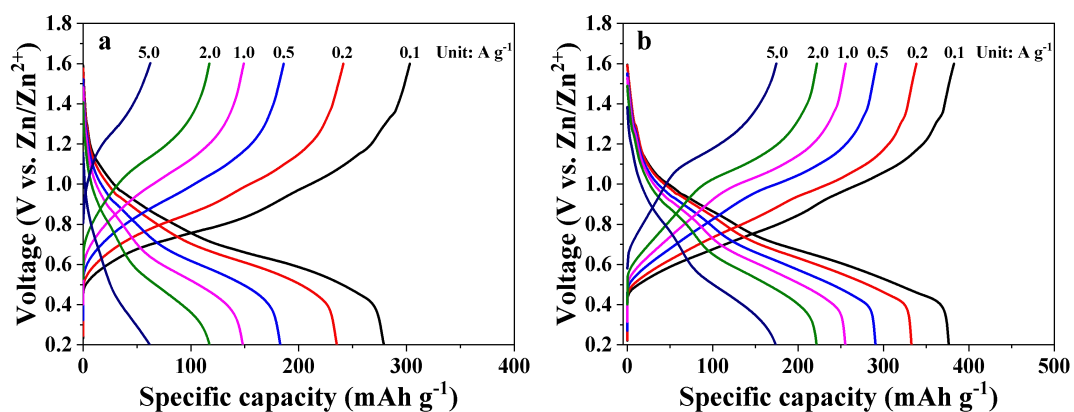


Fig. S6 GCD curves of vanadium oxide bronzes at different current densities: (a) NVO. (b) NCVO.

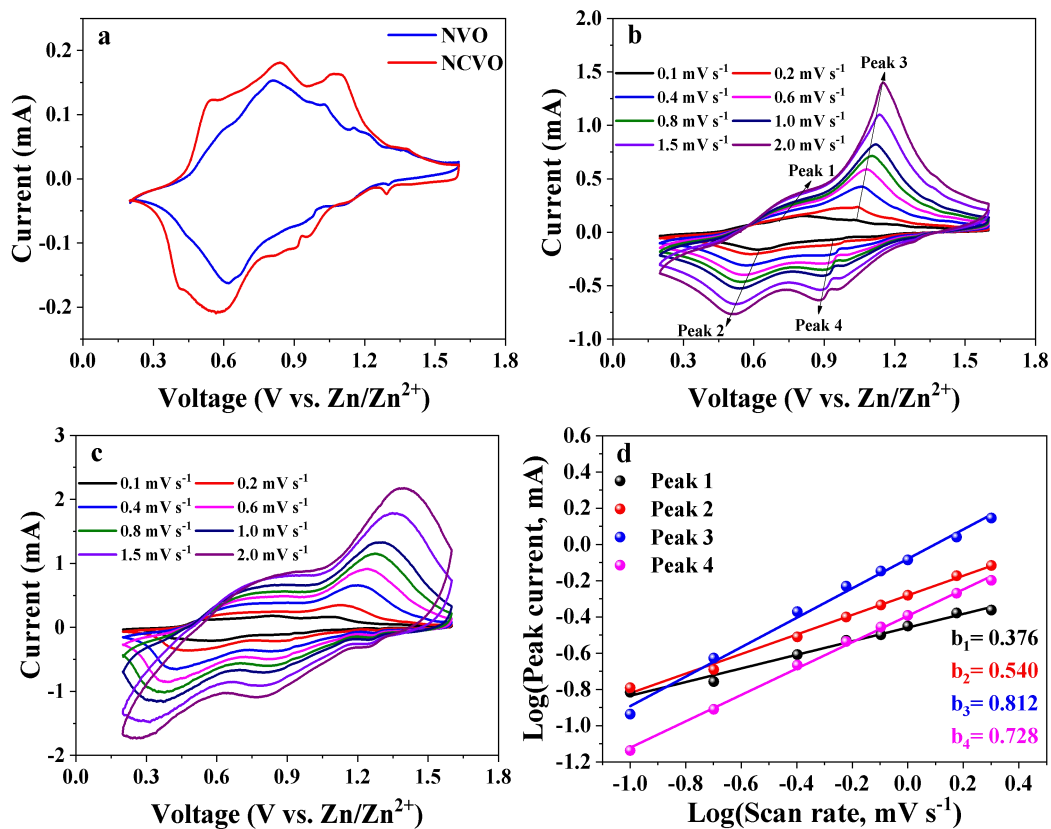


Fig. S7 CV measurements of vanadium oxide bronzes: (a) CV curves of NVO and NCVO at 0.1 mV s^{-1} . (b) CV curves of NVO at various scan rates. (c) CV curves of NCVO at various scan rates. (d) Slope determination of NVO from double logarithmic curves between peak currents and scan rates.

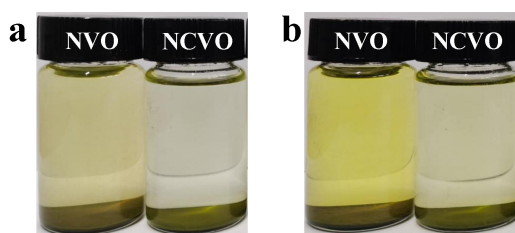


Fig. S8 Digital photographs of vanadium oxide bronzes in 2 M ZnSO_4 aqueous solution over different times: (a) 3rd day. (b) 15th day.

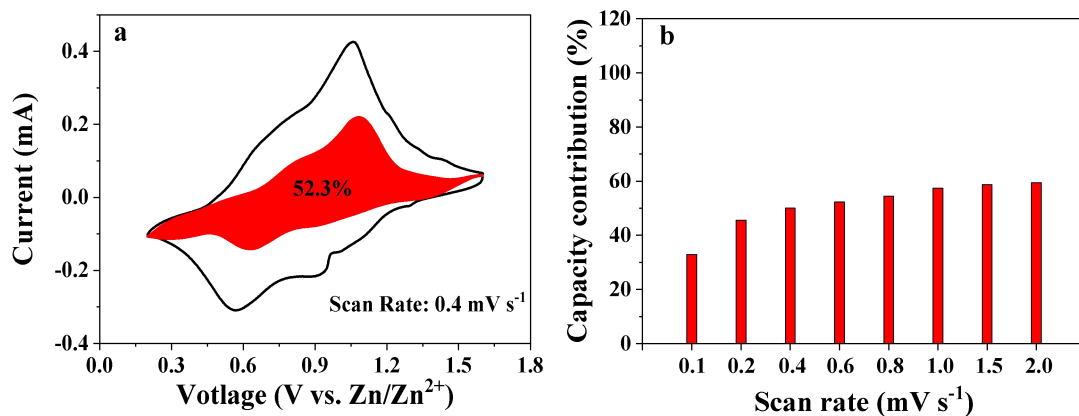


Fig. S9 The electrochemical kinetics analysis of NVO cathodes: (a) Capacitive contribution referred to the red section at 0.4 mV s⁻¹. (b) The contribution proportion of capacitive capacities at different scan rates.

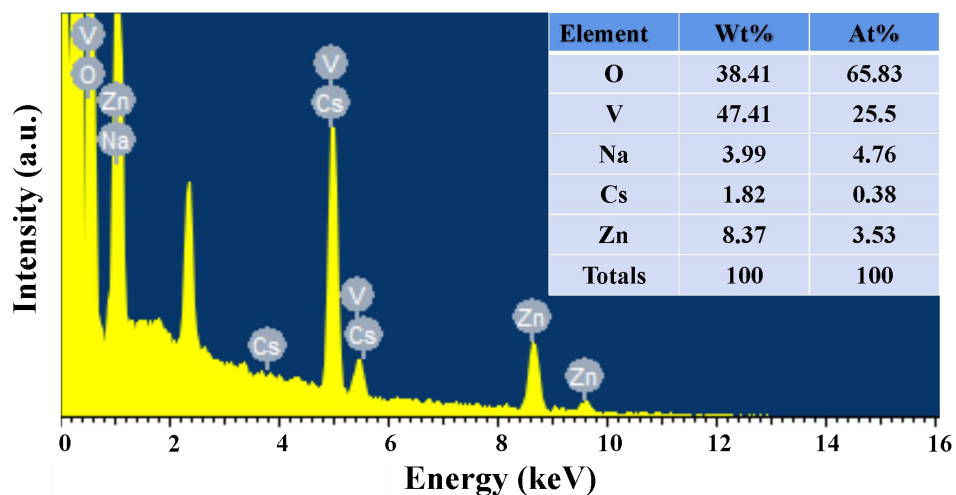


Fig. S10 Corresponding EDS spectrum of NCVO from the element mapping distribution at the full discharge state of 0.2 V for the second charge-discharge cycle.

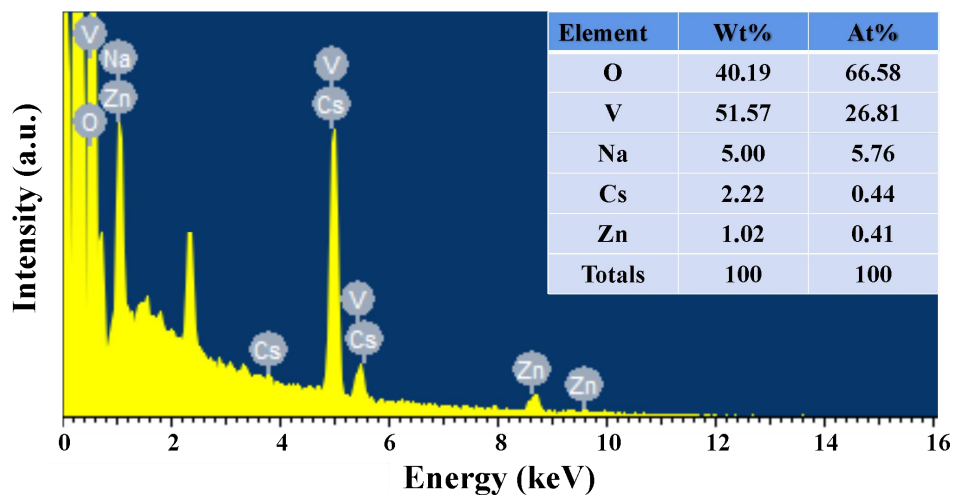


Fig. S11 Corresponding EDS spectrum of NCVO from the element mapping distribution at the full charge state of 1.6 V for the second charge-discharge cycle.

Reference

- 1 J. Li, L. Li, H. Shi, Z. Zhong, X. Niu, P. Zeng, Z. Long, X. Chen, J. Peng, Z. Luo, X. Wang and S. Liang, Electrochemical Energy Storage Behavior of $\text{Na}_{0.44}\text{MnO}_2$ in Aqueous Zinc-Ion Battery, *ACS Sustain. Chem. Eng.* 2020, **8**, 10673-10681.